University of Massachusetts Amherst

ScholarWorks@UMass Amherst

Astronomy Department Faculty Publication Series

Astronomy

2007

The Nonisothermality and Extent of Galactic Diffuse Hot Gas toward Markarian 421

Y Yao

QD Wang
University of Massachusetts - Amherst

Follow this and additional works at: https://scholarworks.umass.edu/astro_faculty_pubs

Part of the Astrophysics and Astronomy Commons

THE NON-ISOTHERMALITY AND EXTENT OF GALACTIC DIFFUSE HOT GAS TOWARD MRK 421

Yangsen Yao[1] and Q. Daniel. Wang[2]
Accepted for publication in the Astrophysical Journal

ABSTRACT

Diffuse hot gas can be traced effectively by its X-ray absorption and emission. We present a joint-analysis of these tracers to characterize the spatial and temperature distributions of the Galactic hot gas along the sight-line toward the nearby bright active galactic nucleus Mrk 421. We also complement this analysis with far-UV O VI absorption observations. We find that the observed absorption line strengths of O VII and O VIII are *inconsistent* with the diffuse background emission line ratio of the same ions, if the gas is assumed to be isothermal in a collisional ionization equilibrium state. But all these lines as well as the diffuse 3/4-keV broad-band background intensity in the field can be fitted with a plasma with a power law temperature distribution. We show that this distribution can be derived from a hot gaseous disk model with the gas temperature and density decreasing exponentially with the vertical distance from the Galactic plane. The joint fit gives the exponential scale heights as ~ 1.0 kpc and 1.6 kpc and the middle plane values as 2.8×10^6 K and 2.4×10^{-3} cm^{-3} for the temperature and density, respectively. These values are consistent with those inferred from X-ray observations of nearby edge-on galaxies similar to our own.

Subject headings: Galaxy: disk — Galaxy: structure — X-rays: ISM — X-rays: individual (Mrk 421)

1. INTRODUCTION

X-ray absorption lines of O VII, O VIII, and/or Ne IX at $z \sim 0$ have been detected unambiguously toward several bright AGNs, but the nature of these highly-ionized species remains uncertain. Because of the limited spectral resolution of the current grating instruments on board the *Chandra* and *XMM-Newton X-ray observatories* (FWHM ~ 50 mÅ, corresponding to a velocity dispersion of 750 km s^{-1} at 20 Å), however, the line width and centroid position do not directly constrain the absorbing gas to be any significantly better than a few Mpc. Some authors have attributed these $z \sim 0$ absorptions to the so-called warm hot intergalactic medium (WHIM) in the Local Group or even beyond (e.g., Nicastro et al. 2002; Rasmussen et al. 2003; Williams et al. 2005). In this interpretation, the hot phase medium could contain large amounts of baryonic matter, accounting for the bulk of the "missing baryons", as predicted in numerical simulations of large-scale structure formations (e.g., Cen & Ostriker 1999; Davé et al. 2001).

But, the $z \sim 0$ O VII, O VIII, and/or Ne IX absorption lines have also been observed in X-ray spectra of the LMC X-3 at distance of 50 kpc (Wang et al. 2005) and many Galactic sources (e.g., Futamoto et al. 2004; Yao & Wang 2005; Juett et al. 2006). The strength of the absorption toward such a source, depending its Galactic coordinates and pathlength, can be substantially greater than those toward the AGNs. A crude characterization of the global distribution of the absorbing hot gas gives an effective scale length of several kpc, suggesting that much of the observed absorptions originates in the Galaxy (Yao & Wang 2005). The recent surveys of AGN spectra with the *Chandra* and *XMM-Newton* archive data show that the O VII absorption line is present in all high quality spectra (McKernan et al. 2004; Fang et al. 2006), indicating a covering fraction of O VII absorbing gas $\gtrsim 63\%$ in the sky. This high covering fraction, together with an estimation of the total mass of the absorbing gas and with a comparison between emission and absorption measurements, further supports the scenario that the X-ray absorbers are primarily associated with the Galaxy (Fang et al. 2006). There is really little doubt as to the presence of the Galactic contribution to the X-ray absorption. The question is how much.

While the line absorption depends on the ionic column density and the dispersion velocity of the intervening hot gas, the emission is sensitive to the number density and temperature of the gas. Therefore a combination of absorption and emission measurements naturally provides a constraint to the scale length of the absorbing/emitting plasma. Rasmussen et al. (2003) and Futamoto et al. (2004) have indeed compared the observed O VII absorption with the background O VII emission line intensity (McCammon et al. 2002) to estimate the scale length of the hot gas around the Galaxy. Similar estimates are also made by Fang et al. (2006). But, so far such estimates all depend on various *assumptions* such as absorption in the linear regime and isothermality of the hot gas, which may not be valid (see §3.1 and §4 for further discussion).

Here we report the first systematic joint-analysis of X-ray absorption and emission data, complemented by a far-UV OVI absorption measurement, in the direction of Mrk 421. The joint-analysis allows for tests of the assumptions and provide tight constraints on our spectral models. Our goals are to characterize both the scale length and global thermal property of the $z \sim 0$ absorbing/emitting hot gas toward Mrk 421.

Throughout the paper, the statistical errors are quoted at the 90% confidence level, unless being pointed out specifically. We also adopt the solar abundance given by Anders & Grevesse (1989) for oxygen[3].

2. OBSERVATIONS AND DATA REDUCTION

2.1. *Chandra X-ray Absorption Data*

[1] Massachusetts Institute of Technology (MIT) Kavli Institute for Astrophysics and Space Research, 70 Vassar Street, Cambridge, MA 02139; yaoys@space.mit.edu
[2] Department of Astronomy, University of Massachusetts, Amherst, MA 01003; wqd@astro.umass.edu

[3] We note that Asplund et al. (2005) proposed a revision of the commonly used solar abundances of Anders & Grevesse (1989), but this revision is still under debate (Antia & Basu 2006). We therefore still use the old values.

ObsID	Obs. Date	Grating/Detector	Exposure (ks)	Used
457	1999 Nov 5	HETG-ACIS	19.83	No
1714	2000 May 29	HETG-ACIS	19.84	No
1715	2000 May 29	LETG-HRC	10.89	No
4148	2002 Oct 26	LETG-ACIS	96.84	Yes
4149	2003 Jul 1	LETG-HRC	99.98	Yes
5171	2004 Jul 3	LETG-ACIS	67.15	Yes
5318	2004 May 6	LETG-ACIS	30.16	Yes
5331	2004 Jul 12	LETG-ACIS	69.50	Yes
5332	2004 Jul 14	LETG-ACIS	67.06	Yes

Mrk 421 is one of the brightest quasars at $z = 0.03$ ($l, b = 179.°83, 65.°03$), and its X-ray flux varies by up to ~ 50 times between quiescent to burst states. Table 1 lists the existing nine *Chandra* observations of Mrk 421, covering various flux levels of the source. Two observations used the High Energy Transmission Grating (HETG; Canizares et al. 2005) with the Advanced CCD Imaging Spectrometer (ACIS-S; Garmire et al. 2003) and the other seven used the Low Energy Transmission Grating (LETG) with either the ACIS-S (five times) or the High Resolution Camera (HRC-S; Murray & Cappell 1986). The LETG provides $\sim 30 - 40$ cm^2 effective area around O VII and O VIII Kα wavelength with a modest resolution of ~ 750 km s^{-1}. Nicastro et al. (2005) and Williams et al. (2005) have reported three (ObsID 1715, 4148, and 4149) of these observations. In this work, we combine six long exposures of these observations to enhance the counting statistics (by $\sim 30\%$); the other three observations, which we do not use, have short exposures, contributing only $< 5\%$ to the total recorded counts around the wavelength of O VII Kα (the most significant absorption line). Furthermore, the LETG-ACIS combination suffers no grating order overlapping complexity as the LETG-HRC does, allowing for a sensitive cross-checking of the measurements between the ACIS-S and HRC-S observations (see below and §4).

We follow the same procedure as described in Yao & Wang (2006) to re-process the individual observations. For the ACIS-S observations, we extract the first grating order spectra and calculate the corresponding response matrix files (RMFs) and auxiliary response functions (ARFs). For the HRC-S observation, we extract the total grating spectrum and calculate the RMFs and ARFs from the first to the sixth grating orders, and then use IDL routines from PINTofALE package[4] to combine all the RMFs and ARFs pairs to form an order-integrated response file accounting for the higher order overlapping in the spectral fitting. To improve the counting statistics, all the spectra, after a consistency check, are then co-added and the corresponding ARFs and RMFs are weight-averaged according to the exposure and global continuum intensity obtained from a model fitting to each spectrum. In the final co-added spectrum, we obtain about 2700 and 1600 counts per channel with a channel width of 12.5 mÅ around wavelength of 18.5, and 21.5 Å, where our interested absorption lines are located.

Our global continuum modeling is conducted in the 2–22.5 Å range. We adopt a power law model with a foreground cool gas absorption to characterize the overall spectral shape of Mkr 421. As in previous studies (Nicastro et al. 2005; Wang et al. 2005), in order to obtain an acceptable

global fit, we include 11 broad ($\sigma > 1500$ km s^{-1}) Gaussian profiles to account for spectral deviations from the adopted power law model and for various calibration uncertainties in detector gap/node regions. The Ne IX, O VIII, O VII Kα, and O VII Kβ absorption lines are clearly visible in their corresponding rest frame wavelength (we do not use other marginally significant $z \sim 0$ absorption lines that have been reported by Williams et al. 2005 and by Nicastro et al. 2005). These absorption lines are characterized with narrow Gaussian profiles in the continuum fit. We obtain a final spectral fit with $\chi^2/d.o.f = 1987/1577$, which, given such high counting statistics, is reasonably acceptable and in particular is good enough for accounting for the higher order overlapping in the LETG-HRC data over the whole wavelength range. The $\chi^2/d.o.f$ in the 12.5-14.5 Å 18.2-20.0 Å, and 20.5-22.5 Å ranges are 202/148, 180/148 and 202/147, respectively.

2.2. *Diffuse X-ray Emission Data*

We use the diffuse 3/4-keV band (R4+R5 bands) background intensity from the *ROSAT All Sky Survey* (RASS; Snowden et al. 1997) to estimate the emission from the hot gas in the field of Mrk 421. The background at lower energies (i.e., 1/4-keV band) is subject to strong absorption by the cool interstellar medium and therefore traces mostly the hot gas within the Local Bubble. The background in the 1.5-keV band is primarily point-like in origin. To avoid any significant contamination from the bright Mrk 421 due to the extended point spread function wing of the *ROSAT*, we use an annulus between $0.°75$ and $1.°75$ radii around the source to obtain a 3/4-keV background intensity estimate as $\sim 1.06 \times 10^{-4}$ counts s^{-1} armin^{-2}. This background intensity contains a significant contribution from unresolved point-like sources. The extragalactic point-like source contribution can be characterized as a power law function with photon index 1.4 and a normalization 10.9 photons s^{-1} keV^{-1} cm^{-2} sr^{-1} at 1 keV (Hickox & Markevitch 2006), which is equivalent to 5.61×10^{-5} counts s^{-1} armin^{-2} in the RASS 3/4-keV energy band (after considering the foreground cool gas absorption $N_H^c = 1.43 \times 10^{20}$ cm^{-2}; Dickey & Lockman 1990). The Galactic component (due to stars) is $\sim 6 \times 10^{-6}$ counts s^{-1} armin^{-2} at the Galactic latitude of Mrk 421 (Kuntz & Snowden 2001). Therefore, we estimate the background intensity due to the Galactic diffuse hot gas as 4.6×10^{-5} counts s^{-1} armin^{-2}. Here we have neglected a potential contribution from charge exchange interactions of solar wind ions with the local neutral interstellar medium (ISM; e.g., Pepino et al. 2004).

The 3/4-keV background is predominantly due to the O VII and O VIII Kα line emission. The best existing spectroscopic measurement of such line emission is from the microcalorimeters flying on a sounding rocket (McCammon et al. 2002) over a region of ~ 1 sr, centered at $l, b = 90°, 61°$, which is at nearly the same Galactic latitude as the Mkr 421 direction and is certainly away from abnormal regions such as the Galactic Bulge, the North Polar Spur, and the Cygnus Loop. The measured line intensities are $I_{\rm OVII} = 4.8 \pm 0.8$ and $I_{\rm OVIII} = 1.6 \pm 0.4$ photons s^{-1} cm^{-2} sr^{-1} (1 σ errors). We assume these intensities are typical for the hot gas at high latitudes. The effects of the foreground cool gas absorption are expected to be small [5] and therefore have not been consid-

---

[4] http://hea-www.harvard.edu/PINTofALE

[5] The neutral hydrogen column density toward the rocket experimental direction is 1.9×10^{20} cm^{-2}. The absorption correction will increase the OVII and OVIII line intensities by 18% and 12% respectively; these changes are comparable to or less than the corresponding 1σ statistic uncertainties.

ered in this work. We use these two line intensities, implemented in a two data point spectrum, to characterize the hot gas emission. This spectrum will be jointly fitted with the absorption data to constrain the emitting/absorbing gas properties, whereas the broadband RASS 3/4-keV intensity will be utilized as a consistency check. We also fake a response file containing two delta functions for this spectrum, so this emission-line-intensity spectrum can be directly compared to our emission line model in the joint analysis.

2.3. *FUSE O VI Absorption Data*

FUSE[6] observed Mrk 421 four times with 29 individual exposures and an actual integrated exposure of 84 ks in total, all configured with the target aperture LWRS ($30'' \times 30''$), providing effective area of ~ 50 cm[2] with spectral resolution of ~ 20 km s^{-1} around the O VI doublet (1032 and 1038 Å).

We only use the data from the LiF1a segment. We calibrate the wavelength for each exposure with CalFuse v3.0[7], and then repeatedly cross-correlate the wavelength scale of different exposures and co-add them to form a final combined spectrum using Don Lindler's IDL Tools[8]. In order to jointly-analyze the *FUSE* and X-ray spectra together in software package *XSPEC*, we transfer the *FUSE* FITS spectrum to a format that can be recognized in *XSPEC*. We adopt a Gaussian line spread function with 20 km s^{-1} (FWHM) as the spectral response of the *FUSE* spectrum.

We use a power law to approximate the continuum and a Gaussian profile to characterize the O VI absorption. We find that one broad Gaussian component is adequate to describe the total absorption. We obtain an EW of the O VI line that is consistent with the previously reported value (e.g., Wakker et al. 2003; Williams et al. 2005). As the line is well-resolved, we measure the dispersion velocity and O VI column density of the absorbing gas as v_b [9] $= 90(84, 97)$ km s^{-1} and $\log[N_{\rm OVI}({\rm cm}^{-2})] = 14.44(14.41, 14.47)$.

3. DATA ANALYSIS AND RESULTS

Our analysis includes the absorption and emission lines of oxygen only to avoid uncertainties in the relative elemental abundances of the hot gas. We assume that the hot gas is in a collisional ionization equilibrium (CIE) state and that the X-ray absorption contains only one velocity component. In reality, each observed line could consist of multiple velocity components. With the still limited spectral resolution of current X-ray data, we decide not to investigate this complexity and leave it to the future when better data become available. The absorption lines of various transients are jointly fitted with our model *absline*[10], implemented in the spectral analysis software *XSPEC*.

3.1. *Isothermal Model*

We first conduct a joint analysis of the O VII Kα, O VII Kβ, and O VIII Kα X-ray absorption lines (Fig. 1). The goodness of the spectral fit with the *absline* model is comparable to that obtained with the Gaussian profiles (§2.1). From the fit, we

obtain the dispersion velocity v_b, O VII column density $N_{\rm OVII}$, and the temperature T of the intervening gas. We can then infer the O VI, O VIII, and hydrogen column densities ($N_{\rm OVI}$, $N_{\rm OVIII}$, and $N_{\rm H}$ respectively) of the absorbing gas (Table 2).
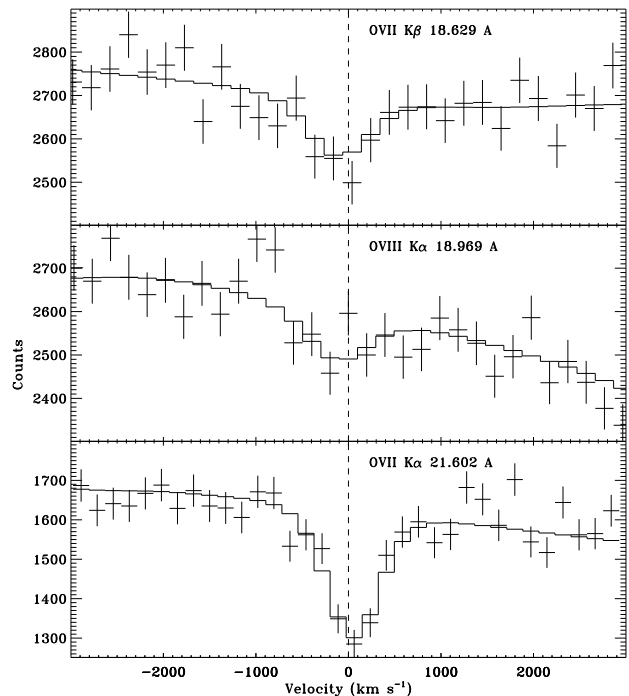

FIG. 1.— The joint fit of the X-ray absorption lines with an isothermal *absline* model. The bin size is 12.5 mÅ; the ARF and RMF have been applied to the model.

We further jointly analyze the O VII emission line intensity (without including the O VIII line; §2.2) with the X-ray absorption lines to estimate the scale length of the emitting/absorbing gas. The oxygen emission line intensity is

$$I[{\rm ph\ cm}^{-2}\ {\rm s}^{-1}\ {\rm sr}^{-1}] = \frac{A_{\rm O}}{4\pi} \int_0^L \Lambda(T) n_e n dl, \quad (1)$$

where $A_{\rm O}$ is the oxygen abundance (in unit of the solar value and assumed to be 1 in the paper), $\Lambda(T)$ is the line emissivity[11], and L is the effective path length of the gas. Assuming that the hydrogen number density can be characterized as

$$n = n_0 e^{-z/(h_{\rm n}\xi)}, \quad (2)$$

where z is the vertical distance away from the Galactic plane, n_0 and $h_{\rm n}$ are the mid-plane value and the scale height, and ξ is the volume filling factor that is assumed to be 1 in the paper, we can integrate Eq. 1 along a sight-line with a Galactic latitude b to get

$$I = \frac{1.2 A_{\rm O} N_H^2 \Lambda(T)}{8\pi L}. \quad (3)$$

Here the factor 1.2 accounts for the helium contribution to the electron density, $L = h_{\rm n}\xi/\sin b$, $N_{\rm H} = n_0 h_{\rm n}\xi/\sin b$. We construct a simple emission line model based on Eq. 3, and use it to model the emission line intensity spectrum we have constructed (§2.2). In the joint analysis, $N_{\rm H}$ and T are the common fitting parameters in both the absorption and emission line models, whereas L only appears in the emission model.

---

[6] For detail description of *FUSE*, please refer to Moos et al. (2000)

[7] http://fuse.pha.jhu.edu/analysis/calfuse.html

[8] http://fuse.pha.jhu.edu/analysis/fuse_idl_tools.html

[9] We use v_b instead of the more generally used b to denote the standard velocity dispersion to avoid the confusion with the Galactic latitude.

[10] For a detail description of the *absline* model and its application in multiple absorption line diagnostics, please refer to Yao & Wang (2005, 2006) and Wang et al. (2005).

[11] The definition of $\Lambda(T)$ is adopted from http://cxc.harvard.edu/atomdb/physics/physics_units/physics_units.html.

	v_b (km s^{-1})	log(T) (K)	log(N_{OVI}) (cm^{-2})	log(N_{OVII}) (cm^{-2})	log(N_{OVIII}) (cm^{-2})	log($N_H A_O$)[a] (cm^{-2})
Isothermal Modeling						
abs.	64(48, 104)	6.16(6.10, 6.21)	13.51(13.32, 13.70)[b]	16.00(15.82, 16.17)	15.18(14.78, 15.41)	19.14(18.98, 19.30)
Non-isothermal Modeling						
abs. + emi.	64(48, 103)	6.44(6.36, 6.54)[c]	14.76(14.53, 14.81)[b,d]	15.99(15.76, 16.04)[d]	15.24(15.01, 15.29)[d]	19.29(19.06, 19.44)
X-ray + FUV[e]	90(83, 96)	6.44(6.37, 6.52)[c]	14.44(14.38, 14.51)[d]	15.86(15.80, 15.93)[d]	15.23(15.17, 15.30)[d]	19.12(19.06, 19.19)

NOTE. — In our absorption line model, the transition oscillation coefficient and the damping factor are adopted from Verner et al. (1996) for O VII and O VIII, and from Morton (2003) for O VI. [a] A_O is oxygen abundance in unit of solar. [b] The model predicated values. [c] The logarithmic value of T_0 at the Galactic plane. [d] These uncertainty ranges can not be directly calculated from the joint analysis, and the error ranges listed here are scaled to have the same ranges as that of N_H. [e] Assuming that all O VI absorptions are associated with O VII-bearing gas. See text for detail.

The obtained N_H and T values are nearly identical to those from fitting the absorption lines alone. In addition, we constrain L to be $\sim 2(0.5, 4)$ kpc. Fig. 2 presents the 68%, 90% and 99% confidence contours of L versus T. However, this isothermal modeling predicts an emission line intensity ratio of $I_{OVII}/I_{OVIII} \gtrsim 20$, in contrast to the observed value of 3 (§2.2). In the isothermal scenario, this ratio depends only on T (Eq.3; Fig. 3). To reproduce this ratio, the temperature needs to be $\sim 10^{6.33}$ K, which is significantly higher than what is inferred from the isothermal model (at $> 99\%$ confidence; Fig. 2). This inconsistency is apparently due to the over-simplification of the isothermality for the hot gas.
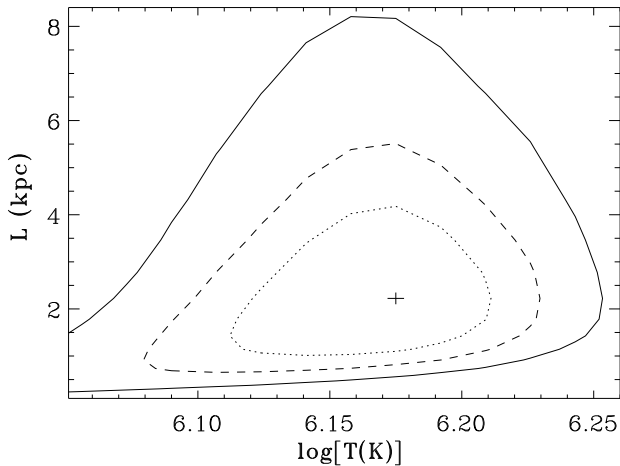

FIG. 2.— The 68%, 90%, and 99% confidence contours of effective scale length (L) versus the temperature (T) of the emitting/absorbing gas at the CIE state, which is obtained by jointly-fitting the O VII (without O VIII) emission line intensity with the observed X-ray O VII and O VIII absorption lines.

3.2. *Non-isothermal Model*

We now consider a simple non-isothermal hot gaseous disk model to interpret the absorption and emission data. This model is motivated by the thick disk-like morphology of diffuse hot gas observed in nearby normal edge-on galaxies and inferred from our statistical sight-line dependence analysis of the Ne IX absorption line (Yao & Wang 2005; Tüllmann et al. 2006; see §4 for the discussion). In addition to the characterization of the density distribution as Eq. 2, the temperature distributions of the hot gas in the disk is assumed to be

$$T = T_0 e^{-z/(h_T \xi)}, \qquad (4)$$

where the mid-plane value T_0 and the scale height h_T, along with h_n and n_0 in Eq. 2, are to be determined. This tem-
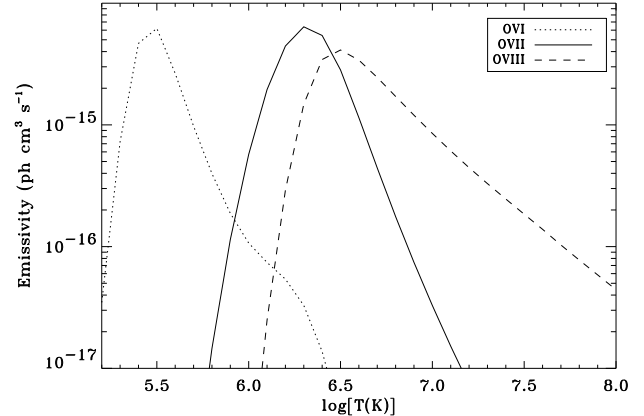

FIG. 3.— The O VI, O VII, and O VIII line emissivities as a function of the gas temperature. The value for O VI has been scaled down by a factor of 1000 for ease of demonstration.

perature distribution is particularly motivated by the apparently lower temperatures of the absorbing gas toward LMC X–3 and Mrk 421 than those toward Galactic sources (Yao & Wang 2005; Wang et al. 2005).

From Eqs. 2 and 4, we can derive

$$n = n_0 (T/T_0)^\gamma, \qquad (5)$$

where $\gamma = h_T/h_n$. Therefore, the differential hydrogen column density distribution is also a power law:

$$\begin{aligned} dN_H &= n dL \\ &= \frac{N_H \gamma}{T_0} (T/T_0)^{\gamma-1} dT. \end{aligned} \qquad (6)$$

The corresponding ionic column density can be expressed as

$$N_i = \frac{N_H \gamma A_e}{T_0} \int_{T_{min}}^{T_0} \left(\frac{T}{T_0}\right)^{\gamma-1} f_i(T) dT, \qquad (7)$$

where A_e and $f_i(T)$ are the element abundance and ionization fraction, and T_{min} is the minimum temperature considered in this work (see below).

Similarly, the surface emission intensity is (Eq. 1)

$$I = \frac{A_e}{4\pi} \int_{T_{min}}^{T_0} \Lambda(T) \frac{dEM}{dT} dT \qquad (8)$$

where

$$\frac{dEM}{dT} = \frac{1.2 N_H^2 \gamma}{T_0 L} \left(\frac{T}{T_0}\right)^{2\gamma-1}. \qquad (9)$$

The intensity can then be calculated for an individual emission line or a broad band with the appropriately chosen Λ.

We modify our *absline* model to accommodate the power law temperature dependence of the absorbing hot gas column density (Eq. 7) and also revise the emission line model constructed in §3.1 according to Eq. 8. We then use these models to jointly fit the X-ray absorption and emission data (including both O VII and O VIII emission lines). We consider the hot gas in the temperature range from $T_{min} = 10^{5.0}$ K to T_0; gas at lower ($< 10^5$ K) temperatures contributes little to the O VI, O VII, and O VIII line absorption/emission. The absorption/emission line joint fit with this non-isothermal model is as good as the one to the absorption lines alone (§3.1). We obtain $\log[T_0(K)] = 6.44(6.36, 6,54)$, $L = 1.8(0.5, 4.5)$ kpc, and $\gamma \lesssim 1.4$. The fitted N_H and v_b values, as included in Table 2, are consistent with those obtained in the isothermal modeling (§ 3.1). But the model predicated O VII/O VIII emission line ratio, 3.7(2.2, 6.7), is now consistent with the observed value.

It is constructive to specify how the individual parameters are constrained, although they are generally correlated in the spectral fitting. The relative O VII Kα to Kβ absorption line strength provides constraints mainly on v_b, N_{OVII}/N_{OVIII} on γ, N_{OVII} on N_H (via the assumed A_O), the emission line intensity ratio I_{OVII}/I_{OVIII} on T_0, and the ratio of I_{OVII} to N_{OVII} on L. Fig. 4(a)-(c) presents the confidence contours of N_H, T_0, and L versus γ. It is clear that although the lower limit to γ is poorly determined here, the L is well constrained to be < 10 kpc at the 99% confident level.

While the X-ray data do not give a tight constraint on γ, the inclusion of the *FUSE* O VI absorption observation in our fit can be helpful. In fact, the above non-isothermal modeling with the X-ray data alone over-predicts the O VI column density by a factor of ~ 2, judged by the best-fitted non-isothermal model (Table 2, §2.3). If the O VI-bearing gas is entirely located in the hot gaseous disk, as prescribed for the X-ray absorption and emission, we can then obtain $\gamma = 0.6(0.4, 0.9)$, $L = 1.8(1.0, 3.2)$ kpc, while the other parameters are included in Table 2 for comparison. The disk model parameters are $\log[T_0(K)] = 6.44(6.37, 6.52)$, $n_0 = 2.4(1.6, 3.7) \times 10^{-3}$ cm^{-3}, $h_n = 1.6(0.9, 2.9)/\xi$ kpc, and $h_T = 1.0(0.6, 1.8)/\xi$ kpc. The confidence contours for N_H, T_0, and L versus γ are presented in Fig. 4 (d)-(f). Compared to Fig. 4 (a)-(c), the tightening is partly due to the directly measured v_b value for the O VI line. Of course, attributing the entire O VI absorption line to the hot gaseous disk represents an extreme case; the relationship between the O VI- and O VII-bearing gases is still very uncertain (see discussion in §4). But, if only part of the O VI absorption is associated with the disk, the lower limit to the γ value will be increased further.

As a consistency check, we further compare the predicted background emission intensity (I_{SXB}) from the characterized exponential disk with the observed value (§2.2). We first revise the thermal emitting gas model *cemekl* (as in XSPEC) and rename it as *absmkl*, [12] which takes T_0, N_H, L, and γ as input parameters and accommodates a power law EM of the gas, as presented in Eqs. 8-9. Taking $L = 2$ kpc, $\gamma = 0.6$, and $\log[N_H(cm^2)] = 19.12$ (Table 2), we integrated this model with RASS response matrix to estimate the expected hot gas emission intensity in the $\frac{3}{4}$ keV band. Since the emission measure is mostly sensitive to the plasma temperature, we include the uncertainty in the mid-plane temperature, $\log[T_0(K)] = 6.44(6.37, 6.52)$ (Table 2). We obtain $I_{SXB} = 1.0(0.4, 1.7) \times 10^{-4}$ counts s^{-1} armin^{-2}, which, within the errors, is consistent with the observed value (§2.2).

---

[12] This model can be obtained from the authors on request.

4. DISCUSSION
4.1. *Comparison with previous works*

We have presented a joint analysis of the $z \sim 0$ absorption and emission lines in the X-ray spectra of Mrk 421 and found that the X-ray absorbing/emitting gas is consistent with being Galactic, most likely located in a thick hot gaseous disk with an effective scale length ~ 2 kpc. This same disk may also explain much of the O VI-bearing gas observed in the far-UV O VI line absorption. Here we compare our results and conclusions with those from existing studies on the hot gas along the same sight-line; some of which also give estimates of the scale length of the X-ray absorbing/emitting gas. All existing studies *assume* that the hot gas along the sight-line is in an isothermal state. We have shown that this assumption is problematic, at least in the Galactic interpretation. Instead, our analysis have allowed for nonthermality, which is facilitated by the joint-fit approach. This approach maximizes the use of the information in the data, and propagates the error of each model parameter and takes care of the correlations between different parameters automatically, and thus yields more reliable results. There are, of course, other differences in both the analysis and interpretation, sometimes leading to very different conclusions in various existing studies.

Rasmussen et al. (2003), for example, estimate a scale length > 140 kpc, based on the averaged O VII and O VIII line absorptions along the sight-lines toward three AGNs (Mrk 421, 3C 273, and PKS 2155-304) and the O VII emission line from McCammon et al. (2002). This estimate uses an ionization fraction f_i of 0.5 for O VII and an oxygen abundance of 0.3 solar. The large scale is in contrast to our inferred value $L \sim 2$ kpc (§3). The bulk of this discrepancy can be easily accounted for (see Eq. 3): oxygen abundance (0.3 solar versus 1 solar), hydrogen density distribution (uniform versus exponential, causing a factor of 2 difference), and the mean hot gas temperature (6.17 versus 6.35 in logarithm, giving a factor of ~ 6 due to the change of both ionic fraction and emissivity). These differences give a combined factor of ~ 40; the different adopted atom data may also contribute. The higher average gas temperature adopted in Rasmussen et al. (2003) results from the inclusion of the 3C 273 sight-line that passes through the inner region of the Galaxy and is apparently contaminated by the North Polar Spur or the radio Loop I (Snowden et al. 1997). Additional difference likely arises from the non-isothermality of our hot gaseous disk model (§3.2). An absorption line tends to be produced by gas at lower temperatures than the corresponding emission line of the same transition (e.g., O VII Kα; compare Fig. 3 and Fig. 1 in Yao & Wang 2005).

Williams et al. (2005) have also compared the $z \sim 0$ X-ray and far-UV (O VI) absorption lines toward Mrk 421, under the isothermal gas assumption. They find that the velocity dispersion inferred from the X-ray absorption lines is smaller than that of the direct measurement of the O VI line. As an alternative, an extragalactic origin of the X-ray-absorbing gas with an inclusion of the photo-ionization process is explored and is found to be consistent with the absorption data, which requires a super-solar abundance ratio of Ne/O. In this work, we only consider the oxygen absorption lines to avoid the uncertainty in the ratio. We find that, while our measured equivalent widths (EWs) for other oxygen lines are consistent with those reported by Williams et al. (2005), the EW of O VII Kα line [11.4(10.20, 12.68) mÅ] is about $\sim 20\%$ higher. Note that our value is consistent with that obtained by Kaastra et al.
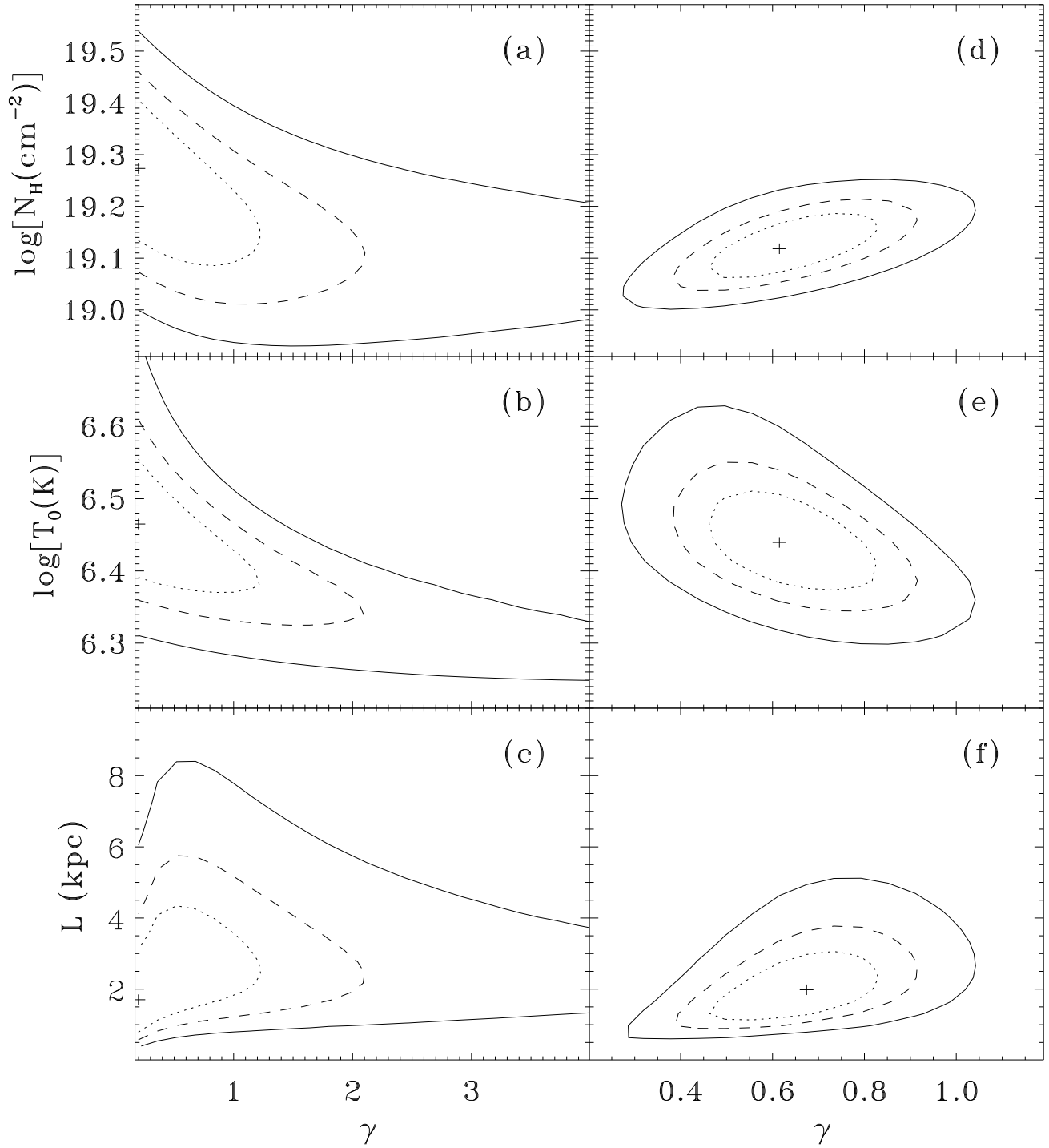
FIG. 4.— The 68%, 90%, and 99% confidence contours of the non-isothermal model parameters. They are obtained from the joint analysis the X-ray absorption/emission data with (right panels) and without (left panels) the inclusion of the far-UV O VI absorption line. See text for details.

(2006). We believe that this discrepancy is mainly due to their improper weighted instrumental response file [13] for the final co-added spectrum; the higher (> 1) order confusion of the HRC observation (if not properly being taken into account), the different placement of the continuum, and the different software packages utilized in the data analysis may also contribute. A higher O VII Kα/Kβ EW ratio indicates a small saturation of the O VII Kα absorption and therefore requires a large b_v, which then becomes consistent with the value of the O VI line. Jointly analyzing the absorption and emission data, we have shown here that the data can be explained by the Galactic hot gas.

Savage et al. (2005) have explored the *FUSE* spectra of Mrk 421 and two nearby stars BD +38°2182 ($l, b = 182°.16, 62°.21$) and HD 93521 ($l, b = 183°.14, 62°.15$) in great detail. They have examined the relationships of the absorption by O VI to those by lowly-ionized species (e.g., H I, C II, C III, and N II) as well as to those by highly-ionized ones (O VII and O VIII). The observed "broad" O VI absorption is divided into the two different velocity components, from -140 to 60 km s^{-1} and from 60 to 165 km s^{-1}. A good correlation between the positive high-velocity O VI component and low ionization gas absorptions is found. Interestingly, the high-velocity O VI component does not seem to show up in the spectra of the two stars. If these sight-lines are not atypical, the positive high velocity absorption should then occur at a distance at least 3.5 kpc off the Galactic plane. In this case, the absorption cannot arise from the same location as the O VII- and O VIII-absorbing gas.

Some portion of the observed O VI absorptions should be associated with the O VII-bearing gas, which we assume to be located in a thick hot gaseous disk. To further probe this association, we reprocessed the *FUSE* observations of BD +38°2182, following the standard CalFuse scripts. We find that the main O VI absorption along the sigh line can be characterized as a narrow component with $v_b = 33(31, 35)$ km s^{-1} and log$[N_{OVI}(cm^{-2})] = 14.20(14.17, 14.22)$. However, because the continuum placement is very arbitrary (see Zsargó et al. 2003 and Savage et al. 2005 for further discussions), this characterization is very uncertain. A careful check suggests that up to 30% of the broad O VI line absorption observed in Mrk 421 can be superposed on the narrow line easily seen in the spectrum of BD +38°2182. This "common" broad component could be associated with the O VII-bearing gas. The remaining O VI line absorptions in the sight-lines toward the star and of Mrk 421 could then arise in the discrete interfaces at boundaries of cool clouds, emersed in hot gas (Savage et al. 2005); the apparent broadening observed in Mrk 421 may be due to the superposition of different velocity components over a large distance. The true absorption and emission of the gas should be a convolution of the local temperature and density dispersions with the global dependences on the off-plane distance. But currently there is little observational or theoretical guidances as to the specific forms of the dispersions. Our simple exponential model, hopefully, provides a first-order correction to the isothermal assumption, or at least demonstrates that the non-isothermality of the hot gas should be seriously explored.

To examine the influence of the "common" component on our results, we perform the same joint analysis as in §3.2, but

requiring the hot gaseous disk accounts for only 30% of the total O VI absorption detected in the Mkr 421 sight-line. The constrained parameter ranges are very similar to those illustrated in Fig. 4 (d)-(f), except for a slightly larger γ and a smaller T_0 values. Clearly, we cannot unambiguously determine the exact fraction of the observed O VI absorption that may be associated with X-ray absorbing gas. But this uncertainty is not expected to qualitatively affect our results and conclusions about the overall non-isothermality and extent of the X-ray-emitting/absorbing gas.

4.2. *Location of the O VII-bearing gas*

The above analysis and results show that the gas that produces the X-ray line absorption and emission along the sight-line toward Mrk 421 is consistent with a Galactic hot thick disk interpretation. But based on the data for this single sight-line, we cannot conclusively determine the location of the gas. As mentioned above, alternative scenarios (i.e. Galactic halo and Local Group) of the $z \sim 0$ O VII-bearing gas have been proposed, allowed for by the limited spectral resolution of the X-ray grating observations. So let us review and discuss the merit and implications of these proposals.

For instance, Nicastro et al. (2002) and Williams et al. (2005) adopted a Local Group WHIM interpretation and found a consistent scale length of ~ 1 Mpc of the gas in the sight lines of PKS 2155-304 and Mrk 421. This consistency is partly a natural outcome of the low-density assumption, hence the importance of the photo-ionization by the extragalactic background in determining the ionic fractions of the gas. This interpretation, however, requires the WHIM to be either metal-rich (e.g., $A_O \geq 0.3$ solar) or severely (spherical) asymmetric (i.e., a small sky-covering-fraction f_c), or both (Williams et al. 2005; Fang et al. 2006), because otherwise the derived total baryonic matter in the Local Group would be even higher than its gravitational mass ($\sim 2 \times 10^{12} M_\odot$; Courteau & van den Bergh 1999). Recently, Fang et al. (2006) performed a systematic search for the O VII absorption line in AGN spectra from archived *Chandra* and *XMM* data and found that the O VII absorption line is detected significantly as long as the counting statistic is reasonably good. They concluded that f_c is $\gtrsim 63\%$ and likely to be unit. This large f_c is clearly contradictory to the requirement of the WHIM interpretation that f_c must be $\lesssim 30\%$ even assuming the solar metallicity for the hot gas (Fang et al. 2006). Therefore, the WHIM scenario is very unlikely, if not impossible, to explain the bulk of the O VII-bearing gas.

Alternatively, hot gas is also expected to be present in the Galactic halo on a scale of ~ 100 kpc. Such a hot gaseous Galactic halo is predicted in galaxy formation theories. Such gas is heated at the so-called virial shocks and through subsequent gravitational compression (e.g., Birnboim & Dekel 2003). This gas, cooling radiatively, can maintain lasting star formation in galactic disks. But simulations tend to overpredict the cooled gas content in galactic disks, which is the so-called "over-cooling" problem (e.g., Navarro & Steinmetz 1997). The inclusion of galactic energy feedback may alleviate the problem, although this has not been satisfactorily demonstrated. Observationally, the existence of a hot gaseous halo around our Galaxy is supported by observations of high velocity (HV; $|v_{LSR}| \gtrsim 100$ km s^{-1}) clouds (HVCs). Some of these clouds, especially compact ones, appear to be located far away from the Galactic plane, although tight distance constraints are very few. The hot gaseous halo may be needed to confine such clouds and may even be their origin through con-
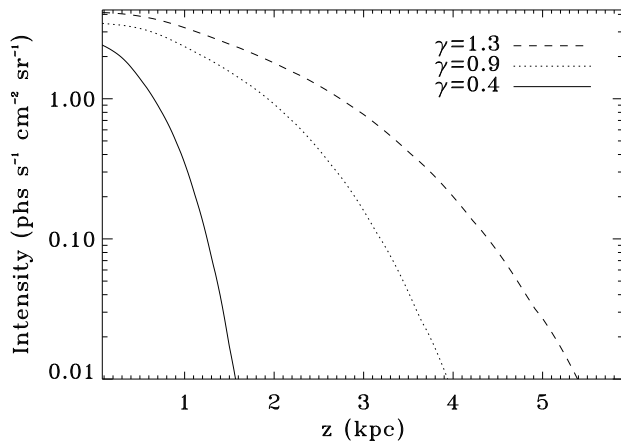

FIG. 5.— The expected surface intensity distribution in 0.3-1.5 keV band as a function of the vertical distance off the Galactic plane.

densation. Furthermore, HV O VI absorption lines are sometimes associated with HVCs and are believed to be produced at their interfaces with the hot halo gas (Sembach et al. 2003). So far, however, there is little observational evidence for a large-scale diffuse X-ray-emitting or -absorbing halo around our Galaxy or other similar disk galaxies (see Wang 2006 for a review), consistent with the conclusion reached in the present work. A scenario that reconciles these observations is that much of the hot halo gas is very low in metallicity, because both the X-ray emission and absorption arise from metal ions. Such a Galactic hot gaseous halo with low metallicity may be a natural product of the strong selective radiative cooling if the accreted gas has a distribution of metal abundances; the gas with a higher metal abundance cools faster and forms denser clouds (probably HVCs), whereas the remaining gas tends to have zero or low metallicity, especially in inner regions of galactic halos. This scenario explains the low X-ray emission/absorption of the hot halo gas and further alleviates the over-cooling problem. A detailed modeling of the scenario will be presented elsewhere.

We favor the interpretation that the bulk of the $z \sim 0$ O VII-bearing gas represents a hot thick gaseous disk around the Milky Way, consistent with previous studies as well as the present one. In this case, the gas represents the hot phase of the ISM and is presumably heated primarily by supernova blastwaves. The presence of the gas is also traced by O VI absorption. As its ionic fraction peaks at 3×10^5 K, O VI is believed to present primarily at interfaces between cool and hot gases and/or in hot gas cooling. The O VI line absorption is observed ubiquitously at relatively low velocity (LV; $|v_{LSR}| \lesssim 100$ km s^{-1}), clearly indicating a predominantly Galactic disk origin (Wakker et al. 2003). The spatial distribution of the O VI absorption indeed has a characteristic vertical scale height of ~ 2.3 kpc around the Galactic plane (Savage et al. 2003) and is thus in a good agreement with that

of the hotter O VII-bearing gas. Therefore, the presence of the hot thick gaseous disk is fully expected and provides a natural explanation for much of the X-ray/far-UV absorption and emission.

The hot thick gaseous disk interpretation is also supported by the X-ray emission observations of nearby disk galaxies like our own. Both the intensity and spatial extent of diffuse X-ray emission appear to be correlated with star formation in galactic disks. Typically the emission is confined to galactic coronae around the disks with vertical extent no more than a few kpc (e.g., Tüllmann et al. (2006), Wang et al. 2003). For ease of comparison with these studies, we present in Fig. 5 the emission intensity distribution as a function of the vertical distance away from the Galactic plane with the best-fit parameters of the hot thick gaseous disk (§3.2). Because the γ is not well constrained, the distribution for several specific γ values are included. For a very broad range of γ, the emission is essentially concentrated within a few kpc off-plane distance. This concentration is consistent with those findings in the nearby disk galaxies (Wang et al. 2003; Tüllmann et al. 2006), suggesting a common behavior and a common nature of hot gas in these galaxies.

To summarize, we have carried out a systematic investigation of the available X-ray O VII and O VIII absorption/emission tracers of Galactic diffuse hot gas in the field of Mrk 421. A joint analysis of the data, complemented by the *FUSE* O VI measurement, enables us for the first time to self-consistently and simultaneously characterize the non-isothermality and vertical scale height of the hot gas in the sight-line toward Mrk 421. We have established that the X-ray-emitting/absorbing hot gas cannot be in an isothermal state. But the X-ray data can be explained with a hot gaseous disk model, which is meant to provide a simple, yet physically plausible characterization of the global temperature and density distributions of the hot gas. Indeed, our inferred scale height of the hot gaseous disk and the gas density at the Galactic plane are consistent with our previous estimations based on the Galactic latitude dependence of Galactic Ne IX line absorptions observed (Yao & Wang 2005).

REFERENCES

Anders, E., & Grevesse, N. 1989, Geochim. Cosmochim. Acta, 53, 197
Antia, H. M., & Basu, S. 2006, ApJ, 644, 1292
Asplund, M., Grevesse, N., & Sauval, J. 2005, ASPC, 336, 25
Birnboim, Y., & Dekel, A. 2003, MNRAS, 345, 349
Canizares, C. R., Davis, J. E., Dewey, et al. 2005, PASP, 117, 1144
Cen, R., & Ostriker, J. P. 1999, ApJ, 514, 1
Courteau, S., & van der Bergh, S. 1999, AJ, 118, 337
Davé, R., Cen, R., Ostriker, J., et al. 2001, ApJ, 552, 473
Dickey, J. M., & Lockman, F. J. 1990, ARA&A, 28, 215
Fang, T., McKee, C., Canizares, C., & Wolfire, M. 2006, ApJ, 644, 174
Fox, A. J., Savage, B. D., & Wakker, B. P. 2006, ApJS, 165, 229

Futamoto, K., Mitsuda, K., Takei, Y., Fujimoto, R., & Yamasaki, N. Y. 2004, ApJ, 605, 793
Garmire, G. P., Bautz, M. W., Ford, P. G., et al. 2003, SPIE, 4851, 38
Hickox, R. C., & Markevitch, M. 2006, ApJ, 645, 95
Juett, A., Schulz, N., Chakrabarty, D., & Gorczyca, T. W. 2006, ApJ, 652, 189
Kaastra, J, S., Werner, N., den Herder, J. W. A., et al. 2006, astro-ph/0604519
Kuntz, K. D., & Snowden, S. L. 2001, ApJ, 554, 684
McCammon, D., Almy, R., Apodaca, E., et al. 2002, ApJ, 576, 188
McKernan, B., Yaqoob, T., & Reynolds, C. S. 2004, ApJ, 617, 232
Moos, H. W, Cash, W. C., Cowie, L. L., et al. 2000, ApJ, 538, L1

Morton, D. C. 2003, ApJS, 149, 205

Murray, S. S., & Chappell, J. H. 1986, SPIE, 597, 279

Navarro, J. F., & Steinmetz, M. 1997, ApJ, 478, 13

Nicastro, F., Zezas, A., Drake, J., et al. 2002, ApJ, 573, 157

Nicastro, F., Mathur, S., Elvis, M., et al. 2005, ApJ, 629, 700

Pepino, R., Kharchenko, V., Dalgarno, A., & Lallement, R. 2004, ApJ, 617, 1347

Rasmussen, A., Kahn, S. M., & Paerels, F. 2003, in The IGM/Galaxy Connection: The Distribution of Baryons at z=0, ed. J. L. Rosenberg & M. E. Putman (ASSL Conf. Proc. 281; Dordrecht: Kluwer), 109

Savage, B. D., Sembach, K. R., Wakker, B. P., et al. 2003, ApJS, 146, 125

Savage, B. D., Wakker, B. P., Fox, A. J., Sembach, K. R. 2005, ApJ, 619, 863

Sembach, K. R., Wakker, B. P., Savage, B. D., et al. 2003, ApJS, 146, 165

Snowden, S. L., Egger, R., Freyberg, M. J., et al. 1997, ApJ, 485. 125

Tüllmann, R., Pietsch, W., Rossa, et al. , 2006, A&A, 448, 43

Verner, D, A., Verner, E. M., & Ferland, G. J. 1996, Atomic Data & Nuclear Data Tables, 64, 1-180

Wakker, B. P., Savage, B. D. Sembach, K. R., et al. 2003, ApJS, 146, 1

Wang, Q. D., Chaves, T., Irwin, J. A. 2003, ApJ, 598, 969

Wang, Q. D., Yao, Y., Tripp, T. M., et al. 2005, ApJ, 635, 386

Wang, Q. D. 2006, the proceedings of Chemodynamics: from first stars to local galaxies, Lyon, France; astroph/0611038

Williams, R., Mathur, S., & Nicastro, F., et al. 2005, ApJ, 631, 856

Yao, Y., & Wang, Q. D. 2005, ApJ, 624, 751

Yao, Y., & Wang, Q. D. 2006, ApJ, 641, 930

Zsargó, J., Sembach, K. R., Howk, J. C., & Savage, B. D. 2003, ApJ, 586, 1019